

# The LOFAR Super Station: An Application of the Hierarchical Design of Phased Arrays for Low-Frequency Radio Astronomy

J. N. Girard <sup>#1</sup>, P. Zarka <sup>#2</sup>, M. Tagger <sup>\*3</sup>, L. Denis <sup>+4</sup>, LSS team

<sup>#</sup> *LESIA, Observatoire de Paris, CNRS, UPMC, Université Paris-Diderot,  
5 place Jules Janssen, 92195 Meudon, France*

<sup>1</sup> *julien.girard@obspm.fr*

<sup>2</sup> *philippe.zarka@obspm.fr*

<sup>\*</sup> *LPC2E, CNRS, Université d'Orléans  
45071 Orléans, France*

<sup>3</sup> *michel.tagger@cnrs-orleans.fr*

<sup>+</sup> *USN, Station de Radioastronomie, Observatoire de Paris, CNRS  
18330 Nançay, France*

**Abstract**—We summarize the technical study conducted in the past 3 years for the definition and prototyping of a hierarchical instrument for low-frequency radioastronomy working in the HF-VHF band: the LOFAR Super Station (LSS). After presenting the concept of the LSS in the context of LOFAR (Low Frequency ARray) instrument, we give an overview of the steps addressed by the design study and the conclusions reached. The main advantage of the LSS in standalone mode will be its very high instantaneous sensitivity, enabling or significantly improving a broad range of scientific studies. It will be a SKA (Square Kilometer Array) precursor and can pave the way for future ground-based instruments on the far side of the Moon.

## I. INTRODUCTION

Low-frequency (LF) radioastronomy has entered a new era with the building of new giant ground-based radiotelescopes. They are designed on phased array technology coupled with advanced signal processing of a large number of antennas. When the number of elementary antennas exceeds the thousand, the realtime processing of all antennas signals becomes intractable even for supercomputers. To reduce the computational load, part of the signal processing is done locally in antenna clusters. These instruments will therefore have a hierarchical design. One example of such instrument is LOFAR (Low Frequency ARray) [1] which is a phased-array interferometer working in the HF & VHF band (30-250 MHz). The whole instrument is composed of 44 radio antennas (or “stations”) distributed all over the Netherlands from a dense central core ( $\emptyset \approx 400\text{m}$ ) with a log-spiral distribution up to  $\approx 600$  km for the international stations built in collaborating countries (Germany, France, Sweden, UK). The longest baseline of the instrument is  $\approx 1500\text{km}$  making LOFAR the first instrument of its kind with an unprecedented sensitivity (down to the mJy level with  $1 \text{ Jy} = 10^{-26} \text{ W}\cdot\text{m}^{-2}\cdot\text{Hz}^{-1}$ ) and angular resolution ( $\approx 1''$ ) in this frequency range. Each station is itself a set of two phased arrays composed of 96 (48 in Dutch stations) elementary antennas working in two separated

bands (to avoid the heavily saturated FM band): the LBA (Low Frequency Antenna - [30,80] MHz) that are inverted-v crossed dipoles and the HBA (High Frequency Antenna - [110,250] MHz) that are  $4\times 4$  analog-phased crossed dipoles “tiles”. The signals of each dual-polarization 96 (48) LBA elements or HBA tiles are preprocessed (filtering, digitization, channelization and beamforming) in a local back-end present at each station. The output signal of each station is sent at 3 Gbits/sec in an optical fiber. The specific design of LOFAR enables the super computer BlueGene/P (University of Gronigen) to gather and handle all signals coming from the stations (by computing either pencil beam and/or interferometric correlations of each inter-station baseline).

At any time, the back-end can connect to either the LBA or the HBA array. However, in the current design of the international station back-end (such as the French “FR606” LOFAR station in Nançay), a third set of analog inputs exists and was initially conceived for a LBL (Low-Band Low - [10-50] MHz) antenna array. These inputs are currently not used by LOFAR for funding reasons. It was proposed to use these available inputs to build a new instrument around the French LOFAR station by connecting a new set of 96 clusters of antennas, representing a total number of  $\approx 2000$  elements. This project is known as the LOFAR Super Station (LSS) [2].

## II. DESIGN OF THE LOFAR SUPER STATION

### A. LOFAR Super Station principle and constraints

The opportunity to use the free inputs of the LOFAR back-end enable to build a new sensitive array of 96 clusters (composed of 10-20 elements) that will create a new LF extension of LOFAR as well as to constitute a new standalone phased array interferometer in Nançay. The advantages of the LSS is to improve the LF instantaneous sensitivity and to extend the frequency coverage (10-90 MHz) of a single 96 LBA array. To remain compatible with the LOFAR back-end,

all LSS operations (element phasing and summing) should be analog. The LSS design is hierarchical and is similar to that of the HBA tiles array in a LOFAR station. The LSS design studies can be decomposed in three steps:

- 1) Element optimization: the element will be an active antenna which geometrical and electrical properties must be optimized for phased array use. It must provide a large primary beam (close to an isotropic antenna) and a large effective area over the 10-90 MHz to extend the instrument field of view.
- 2) Cluster optimization: the number and the relative distribution of the small cluster must be optimized to provide a large beam, a low sidelobe level (SLL) and a improved sensitivity while being compatible with an analog phasing.
- 3) Distribution of clusters: the 96 clusters must be distributed on the Nançay radio observatory to improve both phased array and interferometric characteristic taking into consideration the limited available space and the presence of obstacles.

The following sections will give an overview of the design studies that were carried out.

### B. Optimization of the element

Current and past ground-based instrumental projects for radioastronomy (LWA [3], GURT [4], MWA [5], EMBRACE [6]...) use active elements in their design. Many antenna geometries exist and are fitted for different purposes. Different antenna models were studied through EM simulations with NEC [7]. We studied the impact of the element geometry and electrical environment (variability of both ground conductivity  $\sigma$  and dielectric constant  $\epsilon$ , presence of a ground plane) on the antenna E- and H-patterns, antenna impedance and efficiency. On figure 1 are depicted the parameters that were studied for two main antenna geometries: inverted-v and bow-tie antennas. From these studies, we favored a “thick” inverted-V dipole similar to the LWA Fork [3] antenna (placed 1.5m over a  $3 \times 3$ m metallic ground screen [8],[9]). With this configuration, the antenna has a (classical) half power beam width  $\approx 90^\circ$ (HPBW) at 20 MHz in both E-,H-plane which extends to  $\approx 120^\circ$  at 80 MHz. We discarded log-periodic (Nançay Decameter Array (NDA) antennas [10],[11]) and other “self-similar” antennas because of their large costs despite their frequency independent characteristics [12]. Three different versions of LNA were developed and are currently being extensively tested on antennas in “isolated” (single antenna) and in “cluster” (embedded antenna) regime. They all have good characteristics with a noise  $\sim 10$  dB below the sky noise level but the final choice will depend on tests on the sky.

### C. Design of the cluster

1) Optimization of antenna positions: As compared to classical antenna design looking for an improved directivity, the cluster must have the same properties than a single LSS antenna: it must provide a wide primary beam with a low sidelobe level and a large effective area over the 10-90 MHz

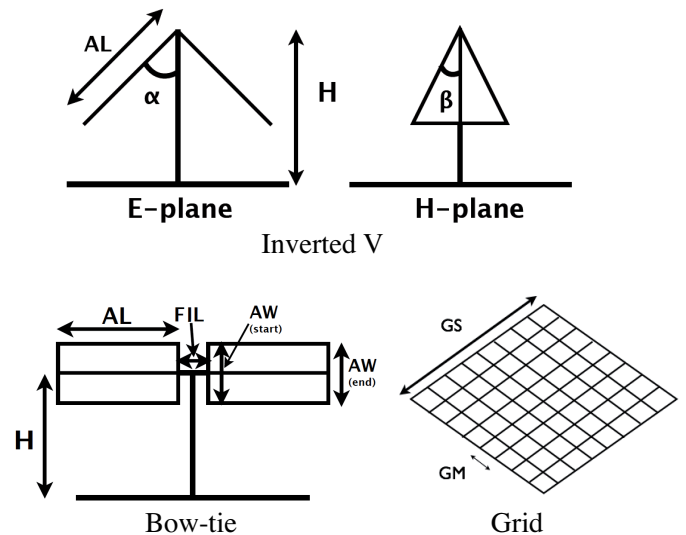


Fig. 1. Geometric parameters considered in the EM simulation with NEC: arm length (AL), arm width (AW), height (H), droop angle  $\alpha$ , apex angle  $\beta$ , grid size (GS), grid meshing (GM). Electrical parameters: conductivity  $\sigma$ , dielectric constant  $\epsilon$  for various types of ground.

bandwidth. Each cluster comes with an analog back-end which role is to phase and sum the element signals so that only one signal (per polarization) is outputted. In parallel to the element design, the study of the number and the relative positions of antennas in a small cluster has been conducted [13]. Two algorithms were used to reduce the SLL:

- 1) an implementation of the Kogan algorithm [14] which propose a deterministic method to reduce the level of the instantaneous most powerful sidelobe in a predefined region by iteratively shifting the antennas on the aperture plane.
- 2) an original implementation based on the simulated annealing [15] algorithm which “thermally” controls the stochastic reduction of the “energy” in the sidelobe region by randomly moving the antennas. The minimized cost function was defined as  $\Omega_m$  [16], the integral of the normalized array beam pattern beyond the primary beam first null. This reduction comes with the increase of the HPBW.

We used two generic antenna patterns in the simulation:  $f_{iso}(\theta, \phi) = 1$  and  $f_{dip}(\theta, \phi) = \cos \theta$  which differ by their extinction at horizon and which account for the beam topology of linear dipoles in both E- and H-planes. A minimal distance between the antennas was determined from effective area overlapping considerations at wavelength  $\lambda$ . We optimized small clusters with a antenna number  $N_{ant}$  from 5 to 22 with initial random distributions. The optimal distributions we obtained with the two methods share similar properties:

- compacity: a dense distribution of antenna in the cluster is equivalent to a filled small aperture which provide, by the Wiener-Khintchine theorem, a wider primary beam.
- irregularity: an irregular cluster will show a lower SLL than that of a cluster showing regularity. This can be

interpreted with an interferometric argumentation on the variety of spatial frequencies that sample the  $(u,v)$  distribution of the cluster. In the extreme case where the cluster is regular, grating lobes (as powerful as the main lobe) will appear at high frequencies.

- pseudo-symmetry: some clusters present circular symmetry and sometimes axial symmetry but are not stackable on themselves by any rotation of angle  $\phi \neq 2\pi$ .

Figure 2 (left) depicts one of the optimized distribution obtained with  $f_{iso}$  that combines the three previous properties. It was obtained for  $N_{ant} = 17$ . From the initial random distribution, the SLL was reduced from -4.8 dBc to -22.6 dBc and the FWHM was increased from  $\approx 13^\circ$  to  $28.8^\circ$  (at  $\lambda$ ) only by optimizing the relative positions of the antennas. Figure 2 (right) represents a regular cluster with  $N_{ant} = 19$  that share common properties with the optimized array with  $N_{ant} = 17$ . Despite the presence of grating lobes, the triangular mesh of the array comes with a triangular distribution of the grating lobes making them less numerous at high frequency as compared to a rectangular mesh [17]. This cluster was the one that was chosen for the three prototypes of cluster in the LSS due to constraints imposed by the analog phasing system. The final distance between antennas was set to 5.5m and results from a compromise between cluster effective area and FWHM.

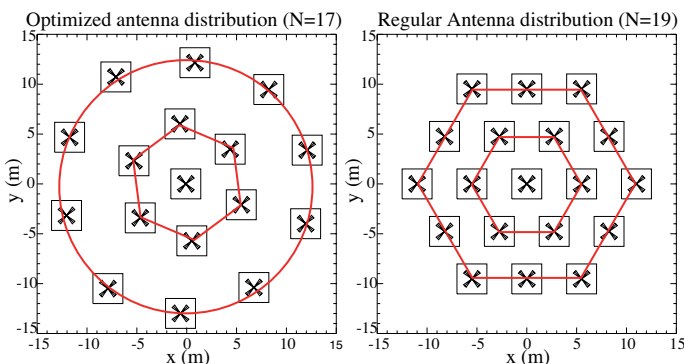


Fig. 2. Minimal distance between antennas is  $d=5.5m$ . (Left) Cluster of  $N = 17$  optimized for low SLL with simulated annealing method. It is composed of a central 6-antenna hexagon and a 10-antenna ring. (Right) Regular array of  $N = 19$  antennas composed of two concentric hexagons.

2) *Cluster phasing*: One of the constraint in the cluster design is the analog phasing. As the cluster back-end must process the signal in an analog way, no digitization is permitted at this level. It is therefore not possible to include digital phase shifters nor tapering strategies by using series of complex coefficients. Moreover, as the cluster should operate in a large bandwidth (10-90 MHz), the phasing must not be chromatic. Therefore we chose to build an achromatic phasing system composed of discretized delay lines similar to what was used for the NDA, for the HBA tiles in LOFAR and for GURT. This kind of technology imposes the array to be partially regular. Moreover, to reduce the amount of cables in the phasing system, antennas are phased by pairs inside the cluster (which allow to use all the cables of the delay lines at any given time). A set of ten 7-bits delay lines was sufficient to phase

the whole cluster of 19 antennas. The lengths of the low loss coax cables inside the delay lines were computed to allow the cluster electronic pointing from zenith to  $\sim 20^\circ$  elevation with a gain variation less than  $\leq 5-10\%$  from a pointing direction to another. The sky was therefore sampled with an angular resolution that spans from  $\sim 0.8^\circ$  (near zenith) to  $\sim 2.5^\circ$  (near horizon) in the  $\theta = [0 - 70^\circ]$  domain.

### 3) *Pressure-driven optimization of the cluster positions*:

The physical footprint of the cluster can be approximated by a disk of radius  $\sim 25m$ . A total of 96 clusters must be distributed within an area of  $\sim 400m$  around the LOFAR station. The LSS will be used as a phased array synthesizing a pencil beam but also as a large interferometer providing baselines from  $\sim 25m$  to  $\sim 400m$  introducing in the same way, new shorter baselines currently absent in LOFAR (which has a minimum baseline of  $\sim 70m$ ). To optimize the distribution of clusters, we used the Boone algorithm developed in [18], which enables the optimization of the visibility density function by considering the  $N_{ant}(N_{ant} - 1)$  visibilities as particles of a gas sensitive to high and low “pressure” gradients which depends on a local excess or lack of visibilities in the  $(u,v)$  plane. From a given  $(u,v)$  density model (which is gaussian for imaging reasons [19]), each antenna will be moved according to the mean pressure force exerted on its associated  $N_{ant} - 1$  visibilities. The algorithm can handle a “site mask” which defined the authorized and forbidden areas where the clusters can be planted. We defined such mask for the LSS (grey and white areas on Fig. 3) taking into consideration the other instruments, the existing underground optical and coaxial network and the channel rill crossing the field. On figure 3, the final optimized distribution of the cluster is shown and possesses a gaussian  $(u,v)$  distribution of  $\sim 400m$  FWHM (represented on the bottom panels). In order to improve the level of sidelobes (especially at high frequency where the cluster response presents grating lobes), each cluster will be rotated by an arbitrary angle to smooth the LSS pattern around the pencil beam.

## III. CONCLUSION

Currently, three prototypes clusters were built in Nançay. They will undergo extensive tests to characterize their performances on the sky. If the concept is validated, the building of the full LSS will start. As other projects of giant ground-based radiotelescopes, the LSS will enhance the capabilities of LOFAR which is designed to unveil for the first time, the last unexplored window accessible from Earth. With an improved sensitivity and high time, spectral and angular resolutions, it address various scientific topics (through “Key Science Projects” from the study of transient radiosources in the solar system (e.g. Jupiter radio emissions) to the observation of cosmological signals (e.g. Epoch or Reionization). Some pioneering projects (such as Farside Explorer) are now considering settling instruments on the far side of Moon for physics and chemical studies of the ground but also for very low frequency radioastronomy (cosmological Dark Ages, slow varying radio sky at decameter-hectometer wavelength...). They can provide information about the conditions and the feasibility of the

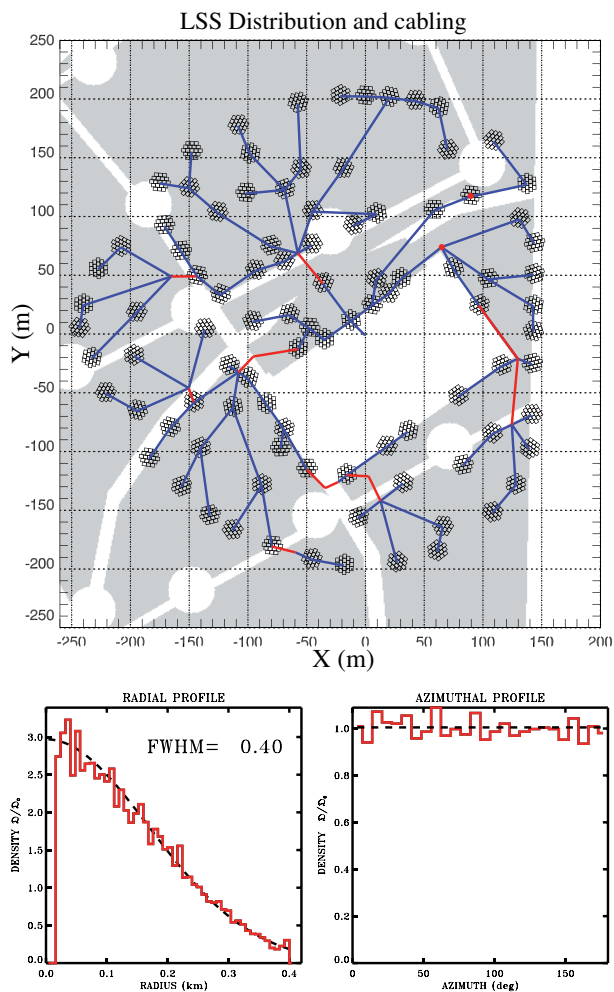


Fig. 3. (top) Distribution of clusters on the Nançay site resulting from (u,v) coverage optimization with the Boone Algorithm [18]). The (u,v) model is a truncated gaussian of 400 m FWHM. The obstacles are taken into account as forbidden placement areas (white) for the clusters. The cable network (blue lines) is the solution of the Cable-Trench Problem [20] in all areas that are thereafter connected together (red dot and lines). Radial (bottom left) and azimuthal (bottom right) normalized density of visibilities associated with the cluster distribution.

potential use of antenna arrays deployed on the Moon surface. This array would operate in a unique environment which is free of any (man-made or natural) source of interference or any cut-off or distortion effects (contrary to the ionospheric cut-off on Earth, below 10 MHz). The design of such array will be extremely challenging because the design constraints of both space-based (limited payload, light and compact elements) and ground-based instrumentation (configuration, phasing and signal retrieving of multiple independent elements) will add up. Rather than using a lot of single antennas, the deployment of small prebuilt antenna clusters (e.g. long patch antennas that unfold on the ground) can be envisaged in future long-range projects on the Moon.

#### ACKNOWLEDGMENT

The authors acknowledge the support of the Observatoire de Paris, the CNRS/INSU, and the ANR (French

“Agence Nationale de la Recherche”) via the program NT09-635931 “Study and Prototyping of a Super Station for LOFAR in Nançay”. The LSS team members is also composed of N. Aghanim, L. Alsac, M. Arnaud, S. Barth, F. Boone, S. Bosse, D. Capayrou, C. Capdessus, B. Cecconi, D. Charrier, A. Coffre, I. Cognard, F. Combes, S. Corbel, N. Cornilleau-Wehrin, P. Cottet, H. Dole, C. Dumez-Viou, C. Ferrari, F. Floquet, S. Garnier, G. Georges, B. Gond, N. Grespier, J.-M. Griebmeier, S. Joly, L. Lamy, M. Lehnert, M. Pommier, P. Sandré, B. Semelin, C. Taffoureau, C. Tasse, E. Thétas, G. Theureau, W. Van Driel, J.-B. Vimont, R. Weber.

#### REFERENCES

- [1] M. de Vos, A. W. Gunst, and R. Nijboer, “The LOFAR Telescope: System Architecture and Signal Processing,” *IEEE Proceedings*, vol. 97, pp. 1431–1437, Aug. 2009.
- [2] P. Zarka, J. N. Girard, M. Tagger, and L. Denis, “LSS/NenuFAR: The LOFAR Super Station project in Nançay,” in *SF2A-2012: Proceedings of the Annual meeting of the French Society of Astronomy and Astrophysics*, S. Boissier, P. de Laverny *et al.*, Eds., Dec. 2012, pp. 687–694.
- [3] S. Ellingson, T. Clarke, A. Cohen, J. Craig, N. Kassim, Y. Pihlstrom, L. Rickard, and G. Taylor, “The long wavelength array,” *Proceedings of the IEEE*, vol. 97, no. 8, pp. 1421–1430, aug. 2009.
- [4] A. A. Konovalenko, I. S. Falkovich, H. O. Rucker *et al.*, “New Antennas and Methods for the Low Frequency Stellar and Planetary Radio Astronomy,” *Planetary, Solar and Heliospheric Radio Emissions (PRE VII)*, pp. 521–531, 2011.
- [5] S. J. Tingay, R. Goeke, Bowman *et al.*, “The Murchison Widefield Array: the Square Kilometre Array Precursor at low radio frequencies,” *ArXiv e-prints*, Jun. 2012.
- [6] G. Kant, P. Patel, S. Wijnholds *et al.*, “Embrace: A multi-beam 20,000-element radio astronomical phased array antenna demonstrator,” *Antennas and Propagation, IEEE Transactions on*, vol. 59, no. 6, pp. 1990–2003, June 2011.
- [7] Numerical electromagnetics code - public domain. [Online]. Available: <http://www.nec2.org/>
- [8] J. N. Girard, P. Zarka, Tagger *et al.*, “Antenna Design and Distribution for a LOFAR Super Station in Nançay,” *Planetary, Solar and Heliospheric Radio Emissions (PRE VII)*, pp. 495–503, 2011.
- [9] J. N. Girard, P. Zarka, M. Tagger *et al.*, “Antenna design and distribution of the lofar super station,” *Comptes Rendus Physique*, vol. 13, no. 1, pp. 33–37, 2012, the next generation radiotelescopes / Les radiotelescopes du futur.
- [10] A. Boisshot, C. Rosolen, M. Aubier *et al.*, “A new high-grain, broadband, steerable array to study jovian decametric emission,” *Icarus*, vol. 43, no. 3, pp. 399–407, 1980.
- [11] Observatoire de nançay. [Online]. Available: <http://www.obs-nancay.fr/en/>
- [12] R. G. Hohlfeld and N. Cohen, “Self-similarity and the geometric requirements for frequency independence in antennae,” *Fractals*, vol. 07, no. 01, pp. 79–84, 1999.
- [13] J. N. Girard and P. Zarka, “Optimization of a small 2d phased array layout synthesizing a wide-beam antenna pattern,” *in prep*, 2012.
- [14] L. Kogan, “Optimizing a large array configuration to minimize the sidelobes,” *Antennas and Propagation, IEEE Transactions on*, vol. 48, no. 7, pp. 1075–1078, jul 2000.
- [15] S. Kirkpatrick, C. D. Gelatt, and M. P. Vecchi, “Optimization by simulated annealing,” *Science*, vol. 220, no. 4598, pp. 671–680, 1983.
- [16] J. Kraus, *Radio astronomy*. Cygnus-Quasar Books, 1984.
- [17] R. Hansen, *Phased Array Antennas*, ser. Wiley Series in Microwave and Optical Engineering. Wiley, 2009.
- [18] F. Boone, “Interferometric array design: Optimizing the locations of the antenna pads,” *A&A*, vol. 377, no. 1, pp. 368–376, 2001.
- [19] —, “Interferometric array design: Distributions of fourier samples for imaging,” *A&A*, vol. 386, no. 3, pp. 1160–1171, 2002.
- [20] F. J. Vasko, R. S. Barbieri, B. Q. Rieksts *et al.*, “The cable trench problem: combining the shortest path and minimum spanning tree problems,” *Computers & OR*, vol. 29, no. 5, pp. 441–458, 2002.